

Tensile Behavior of Single-Crystal Tin Whiskers

S.S. SINGH,¹ R. SARKAR,¹ H.-X. XIE,¹ C. MAYER,¹ J. RAJAGOPALAN,²
and N. CHAWLA^{1,3}

1.—Materials Science and Engineering, School for the Engineering of Matter, Transport, and Energy, Arizona State University, Tempe, AZ 85287-6106, USA. 2.—Mechanical and Aerospace Engineering, School for the Engineering of Matter, Transport, and Energy, Arizona State University, Tempe, AZ 85287-6106, USA. 3.—e-mail: nchawla@asu.edu

The growth of metallic (predominantly Sn) whiskers from pure metallic platings has been studied for over 50 years. While the phenomenon of Sn whiskering has been studied for decades, very little is known about the mechanical properties of these materials. This can be attributed to the difficulty in handling, gripping, and testing such fine-diameter and high-aspect-ratio whiskers. We report on the stress–strain behavior of Sn whiskers inside a dual-beam focused ion beam (FIB) with a scanning electron microscope (SEM). Lift-out of the whiskers was conducted *in situ* in the FIB, and the whiskers were tested using a microelectromechanical system tensile testing stage. Using this technique, the whiskers had minimum exposure to ambient air and were not handled by hand. SEM images after fracture enabled reliable calculation of the whisker cross-sectional area. Tests on two different whiskers revealed relatively high tensile strengths of 720 MPa and 880 MPa, respectively, and a limited strain to failure of ~2% to 3%. For both whiskers, the Young's modulus was between 42 GPa and 45 GPa. It is interesting to note that the whiskers were quite strong and had limited ductility. These findings are intriguing and provide a basis for further work to understand the effect of Sn whisker mechanical properties on short circuits in electronics.

Key words: Sn whiskers, focused ion beam, MEMS, tensile strength

INTRODUCTION

The growth of metallic (predominantly Sn) whiskers from pure metallic platings has been studied for over 50 years.¹ Environmentally benign, Pb-free solders are primarily based on Sn-rich alloys.^{2,3} Thus, a fundamental understanding of whisker growth is important. It is well established that whiskers on Sn platings can grow to lengths exceeding a few hundred microns, and that these whiskers are nearly pure single crystals^{4–6} and possess excellent electrical conductivity.¹ This could result in short-circuiting or interference with other devices.

While the phenomenon of Sn whiskering has been studied for decades, very little is known about the mechanical properties of these materials. Very few studies have been conducted on the mechanical behavior of Sn whiskers.^{7,8} This can be attributed to the difficulty in handling, gripping, and testing such fine-diameter and high-aspect-ratio whiskers. In this work, the objective was to use a reliable means of determining the stress–strain behavior, including the Young's modulus, of Sn whiskers while causing little to no damage. We report on the stress–strain behavior of Sn whiskers inside a dual-beam focused ion beam (FIB) with a scanning electron microscope (SEM). Lift-out of the whiskers was conducted *in situ* in the FIB, and the whiskers were tested using a microelectromechanical system (MEMS) tensile testing stage. Using this technique, the whiskers were not exposed to ambient air and were not handled by hand. SEM images after fracture enabled reliable calculation of the whisker cross-sectional area.

(Received July 23, 2013; accepted February 1, 2014;
published online February 25, 2014)

EXPERIMENTAL PROCEDURES

A sample of pure Sn alloyed with 2 wt.% yttrium was prepared by mixing Sn ingots with Y shot. High-purity Sn-3.9Ag-0.7Cu ingots (Indium, Ithica, NY) were cut into small (6.5 mm × 6.5 mm × 13 mm) rectangular pieces and mixed with Y shot of roughly 2 mm³ to 8 mm³ in size (99.995% pure, packed under argon; ESPI, Ashland, OR). The samples were manually mixed in a crucible in a glovebox, and the mixture was reflowed at 240°C on a hot plate. The microstructure consisted of YSn₃ intermetallic in a pure Sn matrix.⁹ It has been shown that, as the Y phase oxidizes, it causes pure Sn to phase-separate. The Sn is in a state of compression between the Y₂O₃, which results in Sn whiskers being generated.⁹

Figure 1 shows the process by which Sn whiskers were tested. A tungsten needle was welded to a Sn whisker by depositing platinum as a “glue” between the needle and whisker. The FIB was then used to cut the Sn whisker. The needle was moved to the grip in the MEMS device, and Pt was again used to weld the whisker in the grip. The FIB was then used to cut the needle from the whisker. After welding, the whisker was deformed in a quasistatic manner by loading the MEMS stage using a piezo actuator with displacement resolution of 30 nm. The MEMS stage, which is very similar to stages previously used to test freestanding thin films,^{10,11} was fabricated using the process described in Refs. 12,13. The stage has built-in force and displacement sensors that allow simultaneous measurement of nominal stress and strain in the whisker during *in situ* deformation (Fig. 2). Precision alignment of the whisker in the MEMS stage resulted in accurate measurement of the stress–strain behavior. Furthermore, the MEMS stage is designed to ensure uniform uniaxial loading of the whisker and to minimize any bending or torsion that could arise from loading misalignment.¹⁴ During testing, one end of the MEMS stage was fixed and displacement was imposed on the other end in increments of ~150 nm by gradually increasing the voltage on the piezo. After each loading step, the whisker was allowed to relax for 5 min and the elongation and force were recorded. This process was repeated until the whisker fractured. The elongation and force on the whisker were used to calculate the strain and stress on the whisker using its length and cross-sectional area. After fracture, an SEM image of the cross-section of the whisker was taken, and the cross-sectional area was measured using image processing software (ImageJ, Bethesda, MD).

RESULTS AND DISCUSSION

Figure 3 shows surface and cross-section images of a whisker. It is evident that the whisker has a

somewhat irregular shape with striations along the growth axis, which is often observed for extruded whiskers.^{15,16} A SEM image was taken of the fracture surface, being corrected for the 52° angle at which the image was taken to calculate the cross-sectional area. The area of the cross-section was outlined manually using the image-processing software ImageJ, and image segmentation was conducted to quantify the actual cross-sectional area of the whisker (Fig. 4). This area was used in calculations of the stress.

The stress–strain behavior of the whiskers is shown in Fig. 5. The behavior is relatively linear, although some compliance is observed after an initial elastic region of the stress–strain curve. Measurements of the Young's modulus were between 42 GPa and 45 GPa, which is consistent with measurements for pure Sn.^{17,18} Strength values of 720 MPa and 880 MPa were obtained for the two tensile tests. These high strengths are consistent with the fact that Sn whiskers are essentially single crystals. Strain to failure of between 2% and 3% was observed. The variability in the strength and strain to failure is likely the result of preexisting flaws or defects in the whiskers. Energy-dispersive spectroscopy (EDS) analysis on the cross-section of the whisker showed that a negligible amount of oxygen was present on the surface of the whisker. The high strength and limited ductility observed here may possibly be associated with the lack of dislocations in the single-crystal whisker.

Limited studies on the mechanical behavior of Sn whiskers can be found in the literature for comparison with the current work. This can be attributed to the difficulty in handling, gripping, and testing such fine-diameter and high-aspect-ratio whiskers. Powell and Skove⁷ attempted to perform tensile tests on Sn whiskers by carefully removing them from a substrate and gluing the ends with diphenylcarbazine to a pulling apparatus. Force versus displacement curves were obtained, which were linear in nature, although the strength of the whiskers was not reported. Dunn⁸ attempted to obtain the bending stiffness of Sn whiskers using a cantilever method. A large variability in Young's modulus (8 GPa to 85 GPa) was reported. In addition, strength values have been measured by attaching the whisker to a glass slide and turning it vertically to get the whisker to fracture under its own weight. Some potential problems with these data include measurement of the whisker radius with an optical microscope and assuming that the cross-sectional area is circular. Furthermore, in bending theory, the Young's modulus goes as the radius of the whisker to the fourth power, meaning that slight changes in radius could result in large errors in modulus. The technique reported here provides a reliable

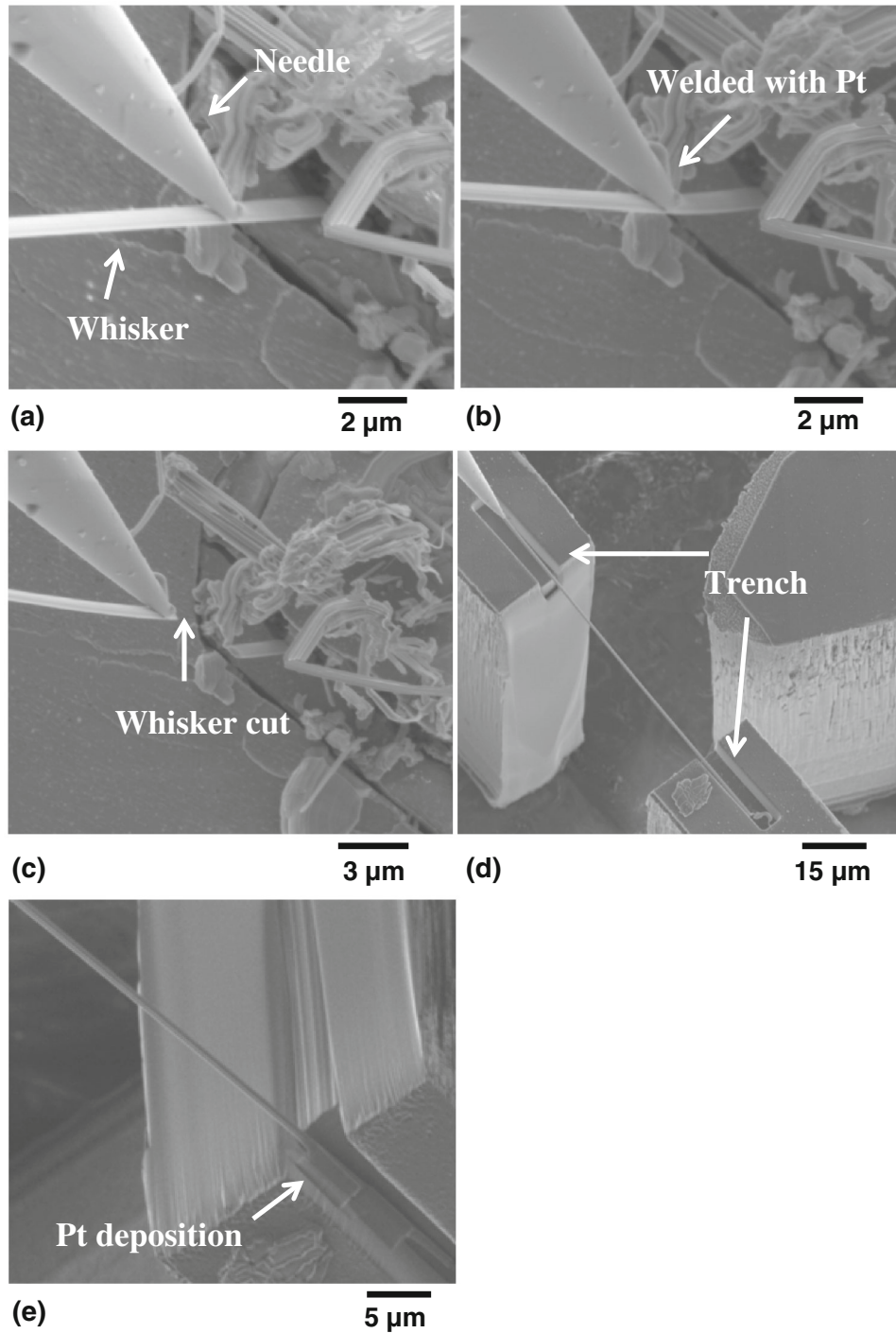


Fig. 1. Process of whisker lift-out and placement on the device inside the FIB/SEM: (a) needle touching the whisker, (b) welding of the whisker to the needle using platinum, (c) cutting the whisker near welded region using FIB, (d) placement of Sn whisker inside the trenches made in the device, and (e) the whisker is welded in place using Pt.

means of determining the stress-strain behavior, including the Young's modulus of the Sn whisker, with little to no damage to the whisker. Furthermore,

since the experiments are done within the SEM, problems with handling, oxidation during testing, etc. can be mitigated.

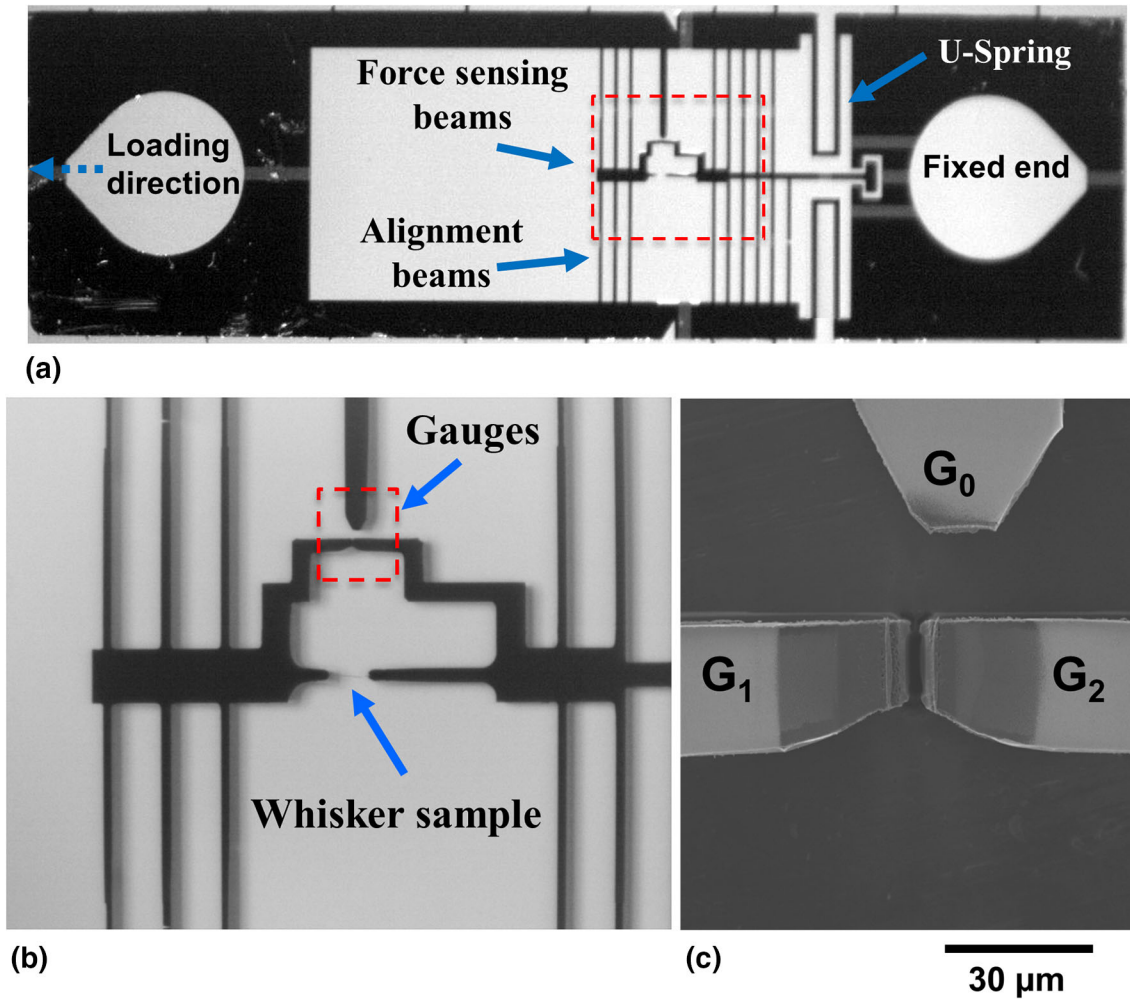


Fig. 2. (a) Optical micrograph of the MEMS stage used for tensile testing of whiskers. When the stage is loaded, the U-springs deform and apply uniaxial tension on the specimen. Alignment beams and U-springs ensure alignment of the sample with the loading axis. (b) Zoomed view of the rectangular box in (a), showing the sample and force and displacement gauges. (c) Scanning electron micrograph of the gauges. During loading, the deflection of the force-sensing beams, provided by the relative displacement of G_1 with respect to fixed gage G_0 , multiplied by their stiffness gives the force on the sample. The elongation of the sample is given by the relative displacement of G_2 with respect to G_1 .

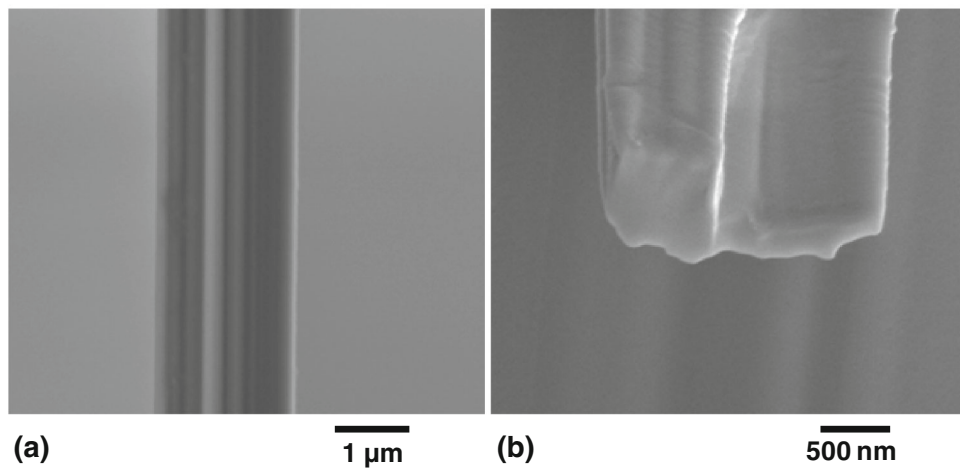


Fig. 3. (a) Top and (b) cross-section views of a whisker; both show the irregular shape of the whisker.

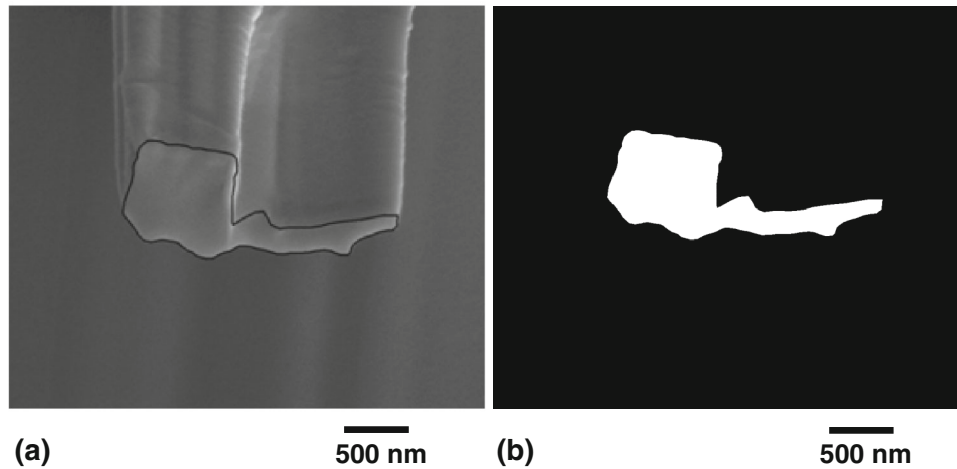


Fig. 4. Measurement of cross-sectional area: (a) line on the boundary of the area, and (b) conversion into binary image to measure the area. The measurement was done in ImageJ (Bethesda, MD).

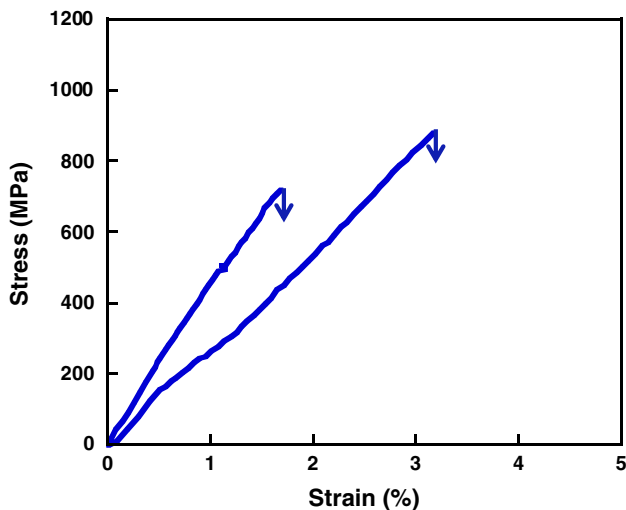


Fig. 5. Tensile stress–strain curves for the Sn whiskers.

CONCLUSIONS

Lift-out of whiskers was conducted *in situ* in the FIB, and the whiskers were tested using a MEMS tensile testing stage to obtain their stress–strain behavior. Using this technique, the whiskers were not exposed to ambient air and were not handled by hand. The tensile strength of the whisker was calculated as 720 MPa and 880 MPa for two tests. The strain to failure and Young's modulus was calculated to be 2% to 3% and 42 GPa to 45 GPa, respectively. It is interesting to note that the whiskers were quite strong and had limited ductility. These findings are intriguing and provide a basis for further work to

understand the effect of Sn whisker mechanical properties on short circuits in electronics.

ACKNOWLEDGEMENTS

We acknowledge the use of FIB-SEM facilities within the Leroy Eyring Center for Solid State Science at Arizona State University.

REFERENCES

1. G.T. Gaylon, *IEEE Trans. Electron. Packag. Manuf.* 28, 94 (2005).
2. S. Mathew, M. Osterman, M. Pecht, and F. Dunlevey, *Circuit World* 35, 3 (2009).
3. 100% Sn plating whisker growth study. <http://www.amd.com>, 10 January 2003.
4. M. Sobiech, M. Wohlschlogel, U. Welzel, E.J. Mittemeijer, W. Hugel, A. Seekamp, W. Liu, and G.E. Ice, *Appl. Phys. Lett.* 94, 221901 (2009).
5. S.-K. Lin, Y. Yorikado, J. Jiang, K.-S. Kim, K. Suganuma, S.-W. Chen, M. Tsujimoto, and I. Yanada, *J. Electron. Mater.* 36, 1732 (2007).
6. J.W. Osenbach, R.L. Shook, B.T. Vaccaro, B.D. Potteiger, A.N. Amin, K.N. Hooghan, P. Suratkar, and P. Ruengsinsub, *IEEE Trans. Electron. Packag. Manuf.* 28, 36 (2005).
7. B.E. Powell and M.J. Skove, *J. Appl. Phys.* 36, 1495 (1965).
8. B.D. Dunn, *Eur. Space Agency (ESA) J.* 11, 1 (1987).
9. M.A. Dudek and N. Chawla, *Acta Mater.* 57, 4588 (2009).
10. J. Rajagopalan, C. Rentenberger, H.P. Karnthaler, G. Dehm, and M.T.A. Saif, *Acta Mater.* 58, 4772 (2010).
11. J. Rajagopalan and M.T.A. Saif, *J. Mater. Res.* 26, 2826 (2011).
12. J.H. Han and M.T.A. Saif, *Rev. Sci. Instrum.* 77, 045102 (2006).
13. J.H. Han, J. Rajagopalan, and M.T.A. Saif, *Proc. SPIE* 6464, 64640C (2007).
14. M.A. Haque and M.T.A. Saif, *Exp. Mech.* 42, 123 (2002).
15. M.W. Barsoum, E.N. Hoffman, R.D. Doherty, S. Gupta, and A. Zavaliangos, *Phys. Rev. Lett.* 93, 206104 (2004).
16. B.-Z. Lee and D.N. Lee, *Acta Mater.* 46, 3701 (1998).
17. X. Deng, M. Koopman, N. Chawla, and K.K. Chawla, *Mater. Sci. Eng. A* 364, 240 (2004).
18. W.D. Callister, *Introduction to Materials Science and Engineering*, 7th ed. (New York: Wiley, 2007).